Available online at www.sciencedirect.com
SCIENCE DIRECT
Polymer 46 (2005) 12093–12102
polymer
www.elsevier.com/locate/polymer

Characterisation of the matrix polymer morphology of polyolefins foams by Raman spectroscopy

M.A. Rodríguez-Pérez [a,*], R.A. Campo-Arnáiz [a], R.F. Aroca [b], J.A. de Saja [a]

[a] Departamento de Física de la Materia Condensada, Facultad de Ciencias, Universidad de Valladolid, C/Prado de la Magdalena s/n, 47011 Valladolid, Spain
[b] Materials & Surface Science Group, University of Windsor, 401 Sunset Ave. Windsor, Ont., Canada N9B 3P4

Received 25 April 2005; received in revised form 19 August 2005; accepted 24 August 2005

Abstract

The spatial resolution provided by micro-Raman spectroscopy is used to probe the morphology of the polymer matrix in a series of closed cell cross-linked polyolefin foams. The experiment set-up allows for the laser beam to be focused with a spatial resolution of 1 μm^2, permitting the structural characterisation of the polymer in the cell faces, cell edges and vertices; i.e. the main constituents which build up the cellular structure of a closed cell foam. The spectra of the solid sheets utilised to produce the foams are used as reference in the discussion of the results for foams. The results have showed a non-homogeneous spatial distribution of the polymer morphology in the foam, which is different from the morphology of the solid sheets. Orientation and phases content are the main sources for these differences.

Keywords: Raman spectroscopy; Polyethylene; Foams

1. Introduction

Closed cell polyolefin foams are two phases materials in which contiguous gas bubbles are entrapped in a macromolecular phase. These heterogeneous materials have found a wide range of applications in different market sectors as for example construction, packaging, buoyancy, automotive, medical, etc. Therefore, the control, optimisation and design of new materials with appropriate physical properties and lower cost are the thrust of the research in this field.

Several studies have been reported on the structure–property relationships of closed cell foams [1–4]. It is widely accepted that the physical properties of given foam depend on several factors [1,2]; among the most important are the foam density, the chemical composition, the polymer morphology and the kind of gas enclosed in the cells. Nowadays, there are more or less detailed studies about the effect of density and chemical composition [1,2]. However, the effect of the cellular structure and polymer morphology has not been completely elucidated.

Different authors have developed theoretical models to predict the mechanical and thermal properties of foams [1,2,5–10]. An important aspect in these models is the foam cellular structure. The cells of low density closed cell foams have, usually, polyhedron shapes. A general accepted geometry for the cells is the Kelvin model (Fig. 1) in which the cells are tetrakaidecahedrons being the three main elements, the cell faces, the cell edges and the vertices. The previous structure has been recently used to compute theoretically the mechanical and thermal properties of foams [11–13].

Additionally, it is also necessary to take into account the properties of the polymer which comprises the cell faces, edges and vertices. For these properties are not known (due to the difficult task of measuring this extremely small parts of the foam structure), and to predict the foam properties, it is assumed that the properties of the same polymer as crystallised in a solid sheet could be used. However, the polymer in the foam could have different morphological characteristics than that of continuous polymers produced by extrusion or injection moulding. Several qualitative arguments can be given in support of this hypothesis:

1. The thickness of cell faces in very low-density foams is around 1–3 μm. These sizes are lower than the typical spherulite dimensions of a low-density polyethylene. As a consequence, a possible influence of the cellular structure on the way in which the foam crystallises may be expected.

* Corresponding author. Tel.: +34 983 184035, fax: +34 983 423572.
E-mail address: marrod@fmc.uva.es (M.A. Rodríguez-Pérez).

0032-3861/$ - see front matter © 2005 Elsevier Ltd. All rights reserved.
doi:10.1016/j.polymer.2005.08.098

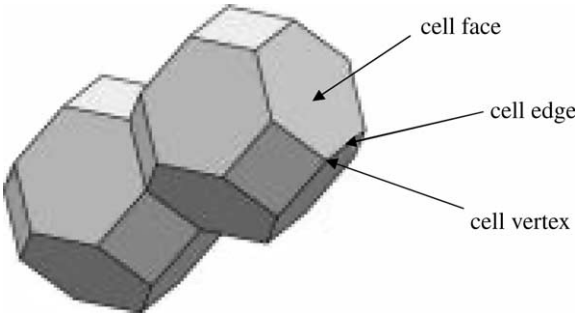

Fig. 1. The main constituents of the structure in a closed cell foam (Kelvin model).

2. The cell edges also have a small thickness (around 10 μm).
3. The polymer in the foam is cross-linked.
4. The polymer is stretched during foaming.

All these features suggest different structural characteristic of the polymer in the foam. This idea has been proposed by several authors [14–17] and has also been at the centre of a few experimental studies [14,17].

Almanza et al. [14] found that the microstructure of the polymer in the cell faces is not spherulitic and they established that the cellular structure and polymer morphology are not independent variables. In fact, the diameter of the supramolecular units which form the structure is conditioned by the cell face thickness. In a similar way, Zipper et al. [17] analysed PP-structural foam mouldings by site-resolved X-ray scattering. The authors showed differences in the microstructure of the foams compared to that of compact injection moulded parts.

There are still several essential questions to be solved in this field, for instance it is not known if cell faces, cell edges and vertices have the same morphology. Furthermore, the orientation and proportion of crystalline phase, amorphous phase and interface of the polymer in single cells has not been studied.

Micro-Raman spectroscopy provides consistent and reliable information about structural and morphological changes in polymeric materials, a characterisation carried down to surface areas of 1 μm^2. As far as we know, this technique has not been used to characterise the morphology of polyolefin foams. The main advantage of using micro-Raman spectroscopy is the possibility for structural characterisation of single cell faces, edges and vertices with an excellent spatial resolution. Previous reports [14,17,18], where the morphology of the polymer in foams has been analysed by diffraction techniques (WAXD and SAXD), used conventional set-ups with beam sizes of several millimetres. Consequently, it was not possible to evaluate the response of single elements and the information obtained was an average for the whole foam.

Here we present the experimental characterisation of a collection of polyolefin foams by micro-Raman spectroscopy. The main objective was the analysis of the spatial homogeneity of the polymer morphology along the different elements of the cellular structure and the study of the morphology of single elements. A direct comparison with the morphology of the solid sheets which were used to produce the foams is also presented, all aiming at a better physical insight into the structure of polyolefin foams.

2. Materials

The product code, base polymer and measured density (ρ) of the materials under study are summarised in Table 1. Four foams, of different densities, were produced from low-density polyethylene (LDPE). One foam based on high-density polyethylene (HDPE), another produced from an ethylene vinyl acetate copolymer (EVA) and a blend of LDPE and HDPE have also been considered. The density of the solid sheets that were used to manufacture the foams is also included in the same table.

These foamed samples are cross-linked closed cell polyolefin foams manufactured by a high-pressure nitrogen gas solution process, and have been kindly provided by ZoteFoams Plc. (Croydon, UK). In this process, a polyolefin is compounded with a peroxide curing agent and extruded as a thick sheet which is passed through a hot oven to effect cross linking (gel content was approximately 40% for all the foams). The characterised solid sheet was taken out from this step of the process. Slabs from the extruded sheet are cut and placed in an autoclave where they are subjected to high pressure (several hundred bars) of nitrogen gas at temperatures above the polymer softening point. Under these conditions, the nitrogen dissolves into the polymer. At the end of the solution stage, and after cooling, the pressure is reduced to zero gauge. The slabs, now containing nitrogen gas for expansion, are placed in a second autoclave under low pressure and again heated above the polymer melting point. Release of the pressure results in full expansion. Finally, the slabs are taken out of the second autoclave and cooled to room temperature. All the foams are subjected to similar cooling conditions.

3. Experimental

Raman spectra presented were recorded in Renishaw systems 2000 and InVia in conjunction with several laser lines. All Raman

Table 1
Main characteristics of the foams under study

Product code	Chemical composition	ρ (kg/m^3)
LD15	LDPE	16.7
LD29	LDPE	30.7
LD33	LDPE	32.0
LD45	LDPE	42.3
HD30	HDPE	23.5
HL34	50% HDPE+50% LDPE	42.6
VA35	EVA (9% VA)	34.2
Solid sheet LDPE	100% LDPE	910
Solid sheet HDPE	100% HDPE	950
Solid sheet HLPE	50% HDPE+50% LDPE	926
Solid sheet EVA	EVA (9% VA)	920

ρ is the foam density.

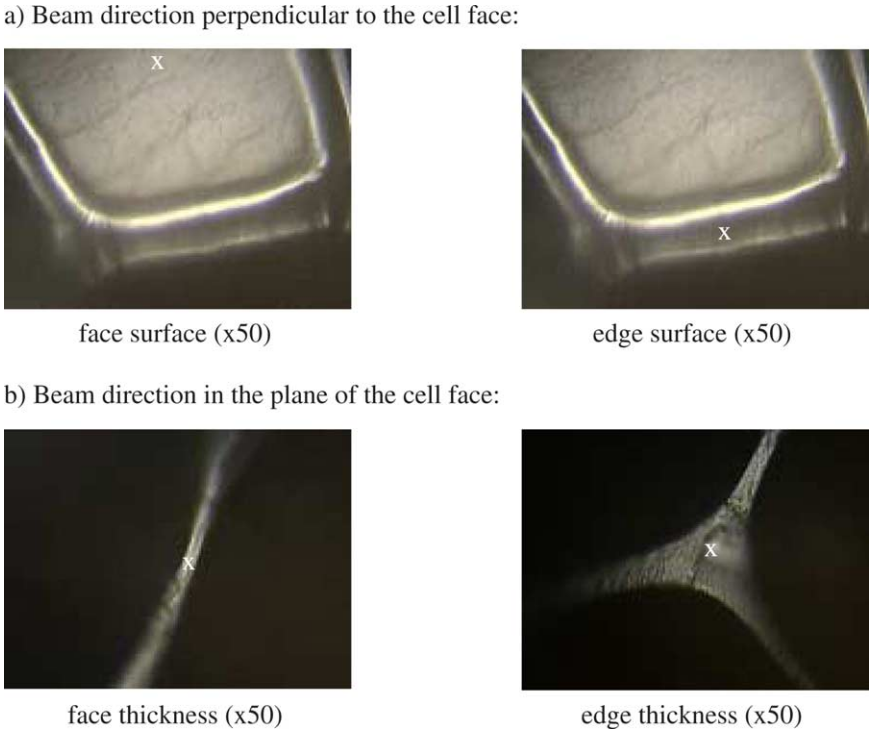

Fig. 2. Experimental set-up in the Raman experiments. Two kinds of experiments were carried out. (a) The laser beam is focused in the parallel direction to the wall. (b) The laser beam is focused in the plane of the cell face.

scattering experiments were conducted with either the Renishaw 2000, or Renishaw InVia systems, using laser excitation at 633 nm He–Ne and the 442 nm laser line from a He–Cd laser and laser powers of 2.5 mW at the sample. The laser beam had circular polarisation. All measurements were made in a back-scattering geometry, using a 50× microscope objective with a numerical aperture value of 0.75, providing scattering areas (spatial resolution) of 1 μm^2. Single point spectra were recorded with 4 cm^{-1} resolution and 10 s accumulation times. Mapping and spatial selectivity in the experiments was achieved using the rastering of a computer controlled 3-axis encoded (*XYZ*) motorised stage, with a minimum step of 0.1 μm.

Experiments were performed with the beam direction perpendicular to the cell face and edge surface (Fig. 2(a)) and with the beam direction on the plane of the cell face and edge surface (Fig. 2(b)). For the first type of experiments, the midpoint point of the face, edges and vertices were chosen (Fig. 2(a)). Spectra were recorded on three cell faces, three edges and three vertices. The average value of these spectra was used to characterise each element of the foam structure. The 95% confidence error of these measurements was ±7% of the average value.

The experiments for the solid sheets were performed with the same experimental set-up. Each solid sheet was measured with the laser beam focused along the three main directions (*XY*, *XZ* and *YZ*). The average spectrum of these experiments has been used to characterise these materials. The 95% confidence error of these measurements was ±5% of the average value.

The spectra were processed with the fitting routine of the Grams Research 2000 software package (Galactic Industries). Voigt line shapes (convolution of Lorentzian and Gaussian bands shapes) and linear baselines were used. Band positions, intensity, FWHH and areas were derived from the curve fitting routine

Other important foam characteristics were measured: cell size (Φ), cell face thickness (δ), mass fraction in the edges plus vertices (f_e), anisotropy ratio (AR), cell shape, melting point (T_m) and crystallinity (X_c). Scanning electron microscopy (SEM) and differential scanning calorimetry (DSC) were used for this purpose. A description of the experimental methods has been published elsewhere [8,14,16].

4. Results

Two levels have to be considered when the structure of polymer foams is analysed. On the one hand, the cellular structure can be studied by using low magnification micrographs (Fig. 3). From these micrographs, cell size homogeneity, mean cell size, anisotropy ratio, mean cell face thickness, mass fraction in the edges, possible residues of foaming agents and overall cell shape can be measured. On the other hand, it is necessary to consider a second structural level, the morphology of the base polymer, which can be studied using a wide variety of techniques (Raman Spectroscopy in this paper). In the next sections the structure of the foams is studied at the two previous levels.

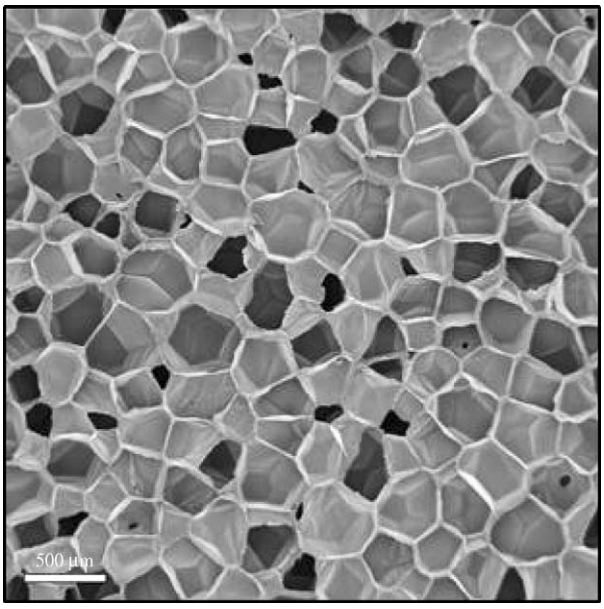

Fig. 3. Low magnification micrograph of the LD45 foam.

4.1. Characterisation of the cellular structure

4.1.1. Cell size distribution and isotropy

The foams under study have an isotropic cellular structure, this can be inferred directly from the micrographs of the cellular structure (Fig. 3 is an example) and from the data on Table 2 (AR ≈ 1). These materials do not present residues from foaming agents in the cell faces. The data for the mean cell size are also collected in Table 2. There is no clear trend for the cell size as a function of the foam density or chemical composition. This is because the nitrogen solution process allows controlling independently density and cell size [11].

4.1.2. Cell face thickness, fraction of mass in the edges plus vertices and average cell shape

The data for the mass fraction in the edges plus vertices and mean cell thickness are summarised in Table 2. All the foams have a non-negligible mass in the edges plus vertices (f_e is around 0.25). The mass fraction in the vertices is around 5–10% of the mass fraction in the edges plus vertices; this estimation was performed from optical micrographs. Therefore a 1.2–2.5% of the mass in the foam would be placed in the vertices.

Table 2
Microscopic characteristics of the foams under study

Foams	Φ (μm)	δ (μm)	f_e	AR
LD15	313	1.4	0.22	1.00
LD29	528	4.2	0.24	1.02
LD33	424	3.6	0.28	1.00
LD45	482	3.9	0.31	0.99
HD30	470	4.5	0.23	1.04
HL34	674	8.8	0.24	0.95
VA35	470	6.1	0.14	1.08

Φ is the mean cell size, δ is the cell face thickness, f_e is the mass fraction in the edges plus vertices and AR is the anisotropy ratio.

The following equation can be used to establish the relationship between the different parameters which characterise the cellular structure [2]:

$$C\delta = (1 - f_e)\Phi\frac{\rho}{\rho_s} \quad (1)$$

where Φ is the mean cell size, f_e is the mass fraction in the edges plus vertices, ρ is the foam density, ρ_s is the base polymer density, δ is the mean cell face thickness and C is a constant that depends on the cell shape. The value of C for the foams under study was 3.79. The two polyehedra with closer values to this one are pentagonal dodecahedrons ($C = 3.46$) and tetrakaidecahedrons ($C = 3.35$) [2]. Therefore, the shape of the cells in these materials is similar to the preceding geometries.

4.2. Polymer morphology

4.2.1. DSC

This technique was used to establish a general trend as a function of density and chemical composition, which, was helpful in the understanding of the Raman results. The values of the crystallinity and melting point for each material are summarised in Table 3. The solid polymer that comprises the cell faces of all LDPE foams has approximately the same melting point and crystallinity. As a function of chemical composition the results are as expected. Melting point and crystallinity follow the same trend:

HD > HL > LD > EVA

4.2.2. Micro-Raman spectroscopy

The Raman spectrum of PE has been extensively investigated and correlations between internal vibrational modes and observed bands have been published [19–22]. The assignment of Raman bands to the different phases in semi crystalline PE samples has been the object of several studies [23–27]. Table 4 lists the Raman shifts of the main vibrations, their internal vibrational modes and the most common assignments to the different phases.

Characteristics fundamental vibrational modes observed between 1000 and 1600 cm^{-1} are frequently used to study morphological structure (e.g. crystallinity, orientation and

Table 3
Thermal characteristics of the foams and solid sheets under study

Foams	χ_c (%)	T_m (°C)
LD15	40.6	105.9
LD29	42.9	108.5
LD33	43.9	105.8
LD45	41.6	108.6
HD30	66.2	130.8
HL34	57.2	127.5
VA35	32.5	92.6
Solid sheet LDPE	41.6	112.8
Solid sheet HDPE	71.1	137.9
Solid sheet HLPE	58.3	134.4
Solid sheet EVA	32.2	97.7

χ_c is the crystallinity and T_m is the melting point.

Table 4
Classification and assignments of Raman bands in PE

Raman shift $\Delta\nu$ (cm^{-1})	Mode	Phase
1064	ν_+ (C–C)	Crystalline + amorphous trans
1131	ν_+ (C–C)	Crystalline + amorphous trans
1170	ρ (CH_2)	Crystalline + amorphous
1295	τ (CH_2)	Crystalline
1305	τ (CH_2)	Amorphous
1370	ω (CH_2)	Crystalline + amorphous
1416	δ (CH_2)	Crystalline
1440	δ (CH_2)	Amorphous trans (interphase)
1460	δ (CH_2)	Amorphous

ν_+, skeletal; τ, twisting; ρ, rocking; ω, wagging and δ, bending.

molecular stress) and can be assigned to the following internal coordinates: the C–C skeletal modes between 1000 and 1200 cm^{-1}, highly sensitive to molecular orientation, stress and conformations; the $–CH_2–$ twisting vibrations characteristically seen around 1295 cm^{-1} which can be used as an internal standard; and the $–CH_2–$ bending modes between 1400 and 1470 cm^{-1} considered to be sensitive to chain packing.

The 1416 cm^{-1} band (CH_2 bending), is thought to be a direct measure of orthorhombic crystallinity and was used by Ströbl and Hagedorn [25] to determine the structural phases of isotropic polyethylene. The method determines the orthorhombic crystallinity phase, amorphous phase and intermediate phase by curve fitting the observed spectrum. The calculation of orthorhombic crystallinity (α_c) is carried out directly using:

$$\alpha_c = 100\frac{I_{1416}}{(I_{1295} + I_{1305} + I_{1269})0.45} \quad (2)$$

where I_{1416} is the 1416 cm^{-1} Raman band area (orthorhombic crystallinity band), $I_{(1295+1305+1269)}$ is the area of the internal standard band group and 0.45 was found through experiments [31].

The amorphous content (α_a) can be calculated from the band at 1303 cm^{-1}

$$\alpha_a = 100\frac{I_{1303}}{(I_{1295} + I_{1305} + I_{1269})} \quad (3)$$

It has been also reported that a simple two-phase model (crystalline phase and amorphous phase) does not provide a complete description of the features observed in PE spectra. The presence of an additional intermediate phase (interface), where chains segments have a preferred trans-conformation without showing regular lateral packing has been confirmed by Raman [25,28], small angle X-ray scattering [29] and NMR measurements [30]. The interface is preferentially located at

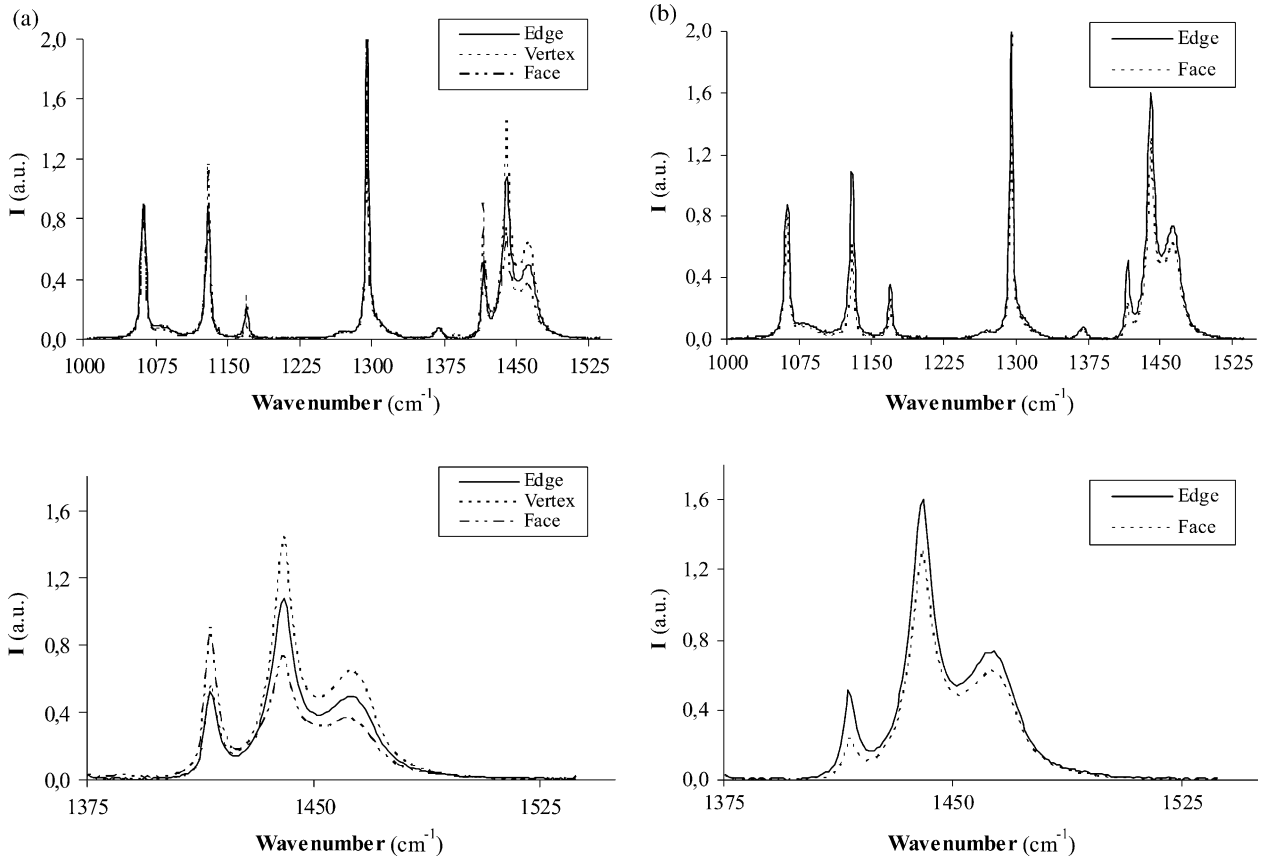

Fig. 4. Raman spectra (sample HD30) in the different foam elements. (a) Experiments performed with the beam focused in the parallel direction to the faces/edges surface and detail in the range 1375–1550 cm^{-1}. (b) Experiments performed with the beam focused in plane of the faces/edges surface and detail in the range 1375–1550 cm^{-1}.

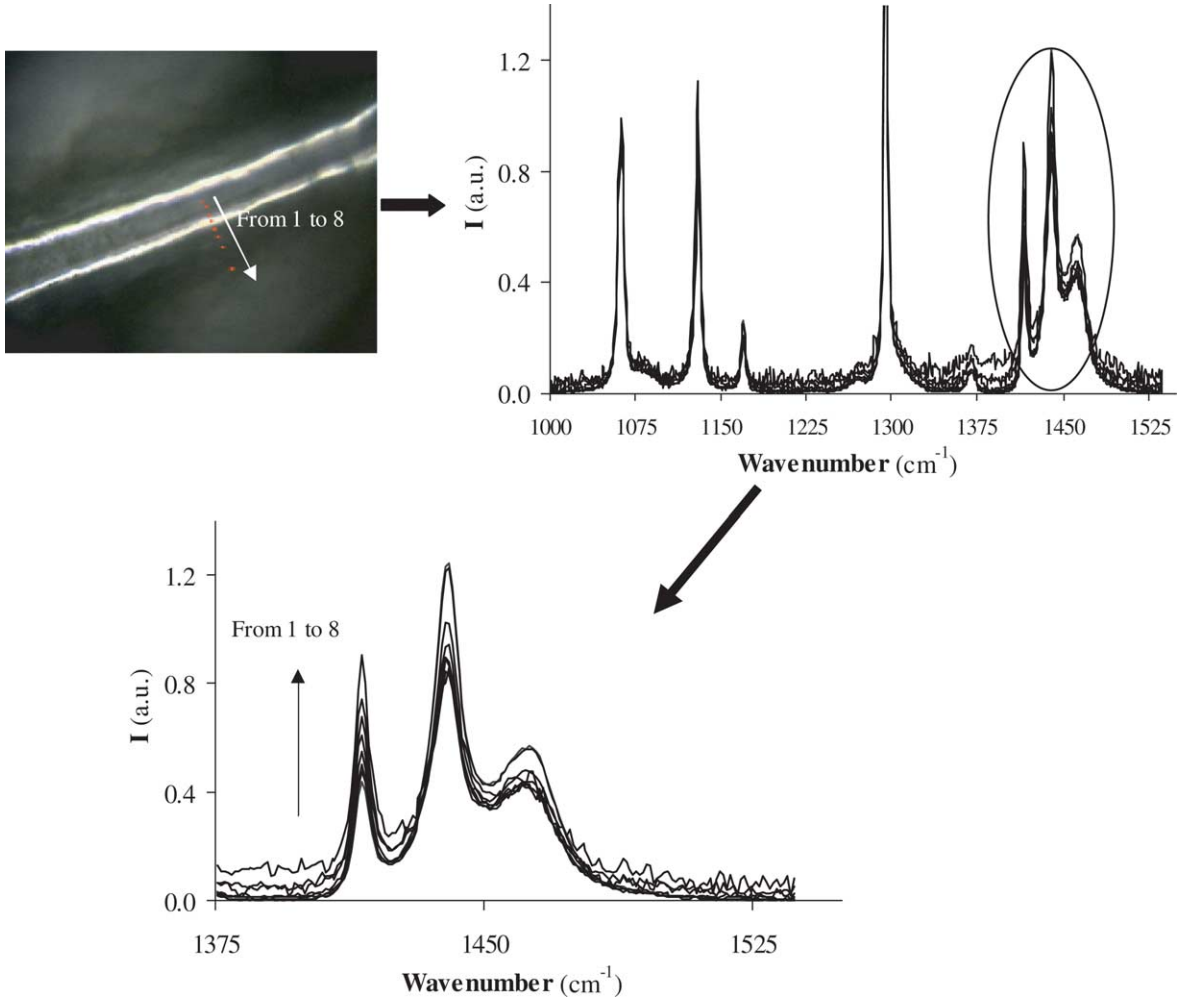

Fig. 5. Mapping experiment for the HD30 foam.

the crystalline fold surface boundary [25,29,31]. The relative amount of interface is given by:

$$\alpha_b = 1 - \alpha_c - \alpha_a \quad (4)$$

Taking into account the previous general information, in this paper the analysis of the Raman spectra has been performed in terms of the crystalline band at 1416 cm^{-1} and the amorphous bands at 1080 and 1305 cm^{-1}.

On the other hand, it is known that, if the phases under analysis (crystalline or amorphous) are oriented, the Ströbl and Hagedorn model, although gives qualitative information about the phases content in the material, can not be used to provide quantitative precise values [32]. As we will see later on, the polymer in the foams is oriented. Due to this reason we term the values obtained applying Eqs. (2) and (3) I_c and I_a to distinguish them with the precise proportion of phases (usually denoted as α_c and α_a). The values of these intensities have been used in the paper to establish comparisons between different zones of the same material or between different materials, not to give quantitative precise values of the phases proportion.

The description of the experimental results is divided in three sections, initially the homogeneity of the polymer morphology is discussed, second the results for the foams are compared to those for the solids sheets, and finally the effect of chemical composition and density is briefly discussed.

4.2.3. Homogeneity of the polymer morphology in the foam

Previous studies [14,18] showed that the polyolefin foams under study crystallised in the orthorhombic phase; other crystalline phases were not present in these materials. Thus, the previous description regarding assignation of Raman bands could be directly applied to these materials.

The Raman spectra of the faces, edges and vertices (measured with the beam direction perpendicular to the cell face and edge surface), for the HD30 foam in the internal modes region is shown in Fig. 4(a). A qualitative comparison brings the attention to the considerable differences observed in the 1416 cm^{-1} band; this band is much more intense in the face, similar results are attained for edges and vertices. Small differences are also detected for the amorphous band at 1080 cm^{-1}.

The Raman spectra for the same material measured in the parallel direction to the face surface showed a different

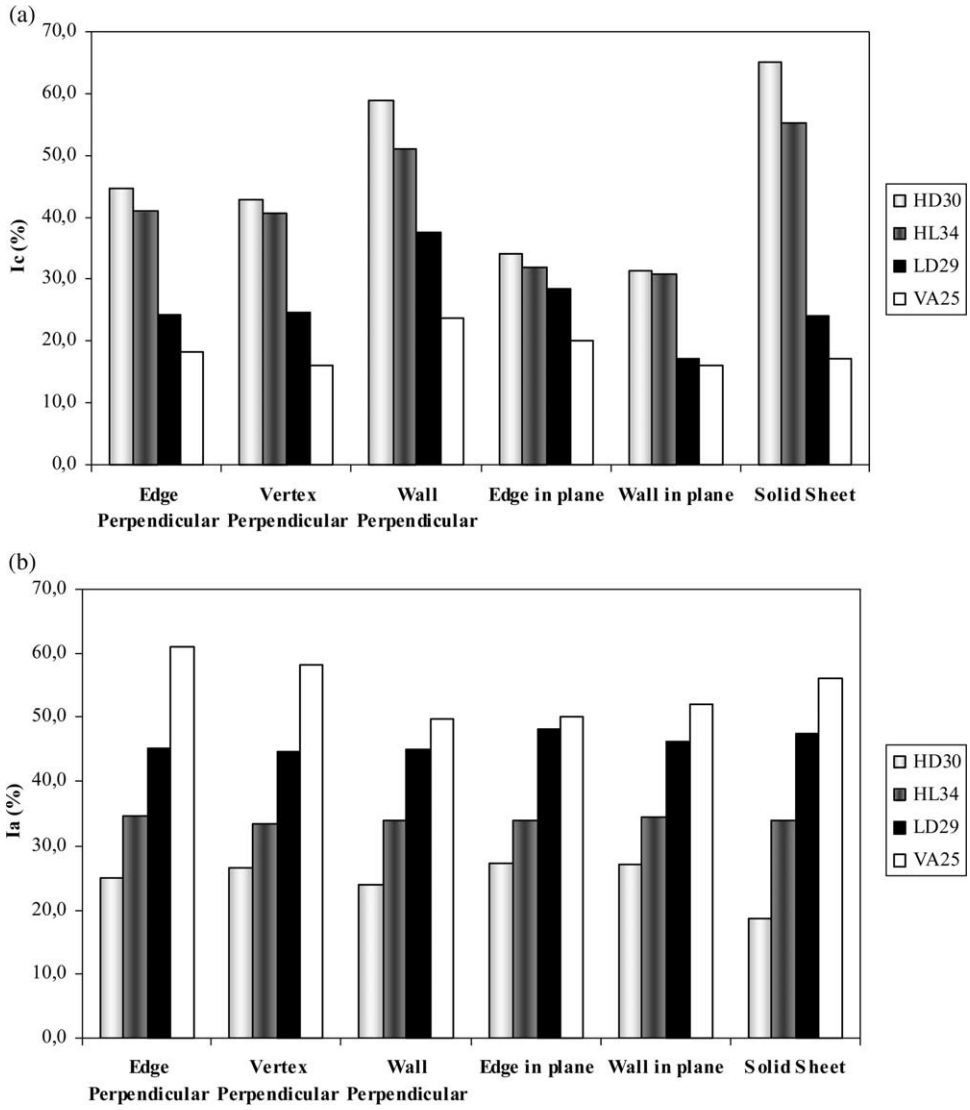

Fig. 6. Relative intensity of the crystalline (a) and amorphous (b) band for foams of similar density and different chemical compositions and for the solid sheets.

behaviour (Fig. 4(b)). The crystalline band measured in the faces is slightly less intense than that measured in the edges.

The previous trend can be clearly observed in the mapping experiment described in Fig. 5. The beam was initially focused on the surface of and edge (point 1 in the figure), and then slightly moved to different points from the edge to the adjacent face (from point 1 to 8). The intensity of the characteristic crystalline band at 1416 cm^{-1} increases considerably when the face is reached.

Differences in intensities for experiments performed in different directions can be explained in terms of the orientation of the polymer chains. Cell faces and edges are biaxial stretched during foaming, as a consequence the polymer chains in the crystalline phase have a preferential orientation which is detected in the Raman spectra. The results seem to indicate that faces and edges are stretched in a different extend, being the stretching more intense in the faces.

The foam HL34 and the HL solid sheet are blends of LDPE and HDPE. It is expected that a blend of these two immiscible polymers give rise to a two phases material (LDPE phase and HDPE phase), each phase with a different morphology and as a consequence different Raman spectrum. However, the Raman experiments through the materials did not detected the two components, indicating that the domains size is below the spatial resolution of the experiments (1 μm^2).

To compare between foam elements, the relative intensities of the bands at 1416 cm^{-1} (I_c) and 1303 cm^{-1} (I_a) were calculated following the Ströbl and Hagedorn model (Eqs. (2) and (3)).

Fig. 6(a) shows the results for the faces and edges of foams with a similar density and different chemical compositions, the results for the solid sheets are also included. It can be observed the previously mentioned trend that shows that the relative intensity of the crystalline band is much higher for the faces when the experiments are performed with the beam direction perpendicular to the cell face and edge surface and is slightly higher for the edge when the experiments are performed with the beam direction on the plane of the cell face and edge

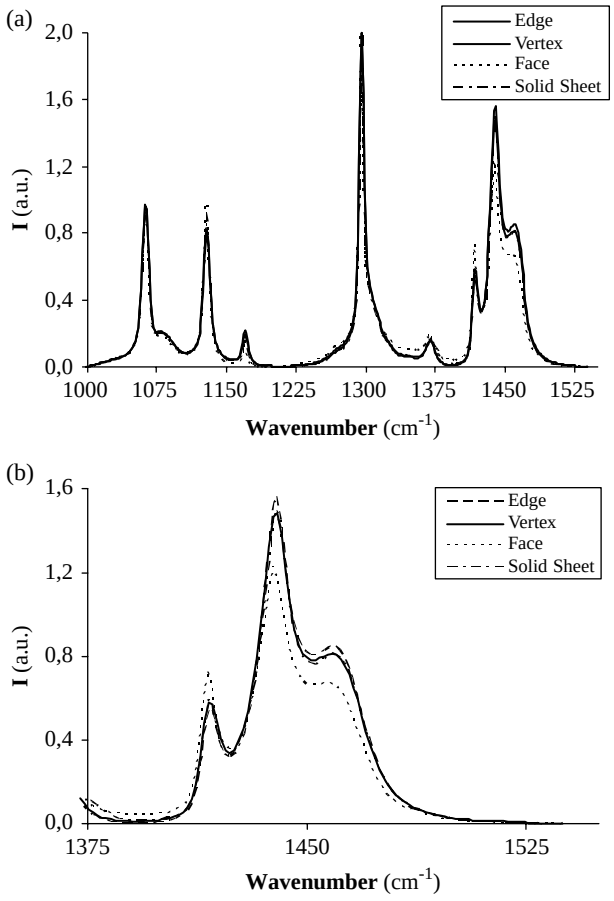

Fig. 7. Raman spectra for the LD15 foam (perpendicular direction) and for the LD solid sheet. Detail of the spectra in the range 1375–1550 cm^{-1}.

surface. This is a general tendency observed for all the foams studied, although the differences are more significant for materials of higher crystalline content (HD30 and HL34 foams).

In the case of the amorphous band (Fig. 6(b)), the variations between measurements in the plane of the face and in the perpendicular direction do not show a clear trend. It seems that the intensity of this band is almost independent on the measuring direction for all the elements of the foam structure and, in addition, the intensity of this band does not depend on the foam element (i.e. the spatial distribution of this band is constant).

It is well known that chain entanglement and other topological constraints hinder sample drawability. For stretched polymers, crystals are thought to remain oriented after the stress ceases, whereas the amorphous phase is thought to recoil. Accordingly, an almost isotropic amorphous phase for all the materials and a higher molecular orientation in the crystalline phase for the samples with higher crystallinity should be expected. This concept is corroborated by the former results. The same result has been found, for instance, for cold-drawn polyethylenes [32], in these materials the crystalline phase is oriented during stretching, and however, the amorphous phase remains isotropic after the drawn process.

4.2.4. Comparison to the solid sheets

Fig. 7 shows the Raman spectra of the LDPE solid sheet (average of the experiments performed in three perpendicular directions) compared to that measured in different elements of the LD15 foam (experiments in the perpendicular direction). The spectra of the solid sheet (results not shown) were almost independent of the measurement direction, indicating a smaller degree of orientation in this material. The same trends observed for the HD30 foam are also characteristic of the LD15 material, although the differences between the foam elements are smaller in this last foam. It is also obvious that the Raman spectrum of the solid sheet is similar to that of the edges and vertex and completely different to that of the cell faces.

A quantitative comparison between foams and solid sheets can be seen in Fig. 6. The amorphous band for the foam elements and for the solid sheets is similar; however, the crystalline band presents several remarkable differences. For the materials of lower crystallinity (LD and VA) the intensity of the crystalline band in the sheet is comparable to that of the edges and vertex and smaller than that of the faces measured in the perpendicular direction. However, for the materials with higher crystallinity (HD and HL), the relative intensity of the crystalline band is clearly higher in the solid sheet than in any foam element.

Therefore, the polymer morphology in foams of similar densities appears to have different characteristics depending on the chemical composition. On the one hand, the foams produced from branched polymers, for instance LDPE or EVA copolymers, in which the crystallisation is restricted by topological constraints, have a polymer morphology in faces and edges that, in terms of the intensity of the crystalline and amorphous bands, seems to be similar to that of the solid sheet from which the material is produced.

On the other hand, the foams produced from more linear polymers, high density polyethylene or blends of HDPE and LDPE, have a crystalline band which is smaller than that of the sheets, indicating that the processing, and the different modifications that the polymer undergo during foaming (crosslinking, stretching, crystallisation, etc), could restrict the ability to crystallise in these more crystalline foams, giving a microstructure with a smaller crystalline content and a higher interface content in comparison with the solid sheet. Crystallinity measured by DSC support this hypothesis, slightly higher crystallinities are measured in the solid sheets of the HD and HL materials.

Other possible contribution to this behaviour of the crystalline band could be related to the presence in the foams of an ill-defined orthorhombic crystalline structure (with an important disruption of the orthorhombic crystals), which it is known reduces the intensity of the I_{1416} band. This kind of ill-defined structure has also been detected in cold-drawn high density polyethylenes [32].

4.2.5. Effect of chemical composition and foam density

Fig. 6 shows that both the relative intensities of the crystalline and amorphous bands follow the expected trend which was found by differential scanning calorimetry (DSC).

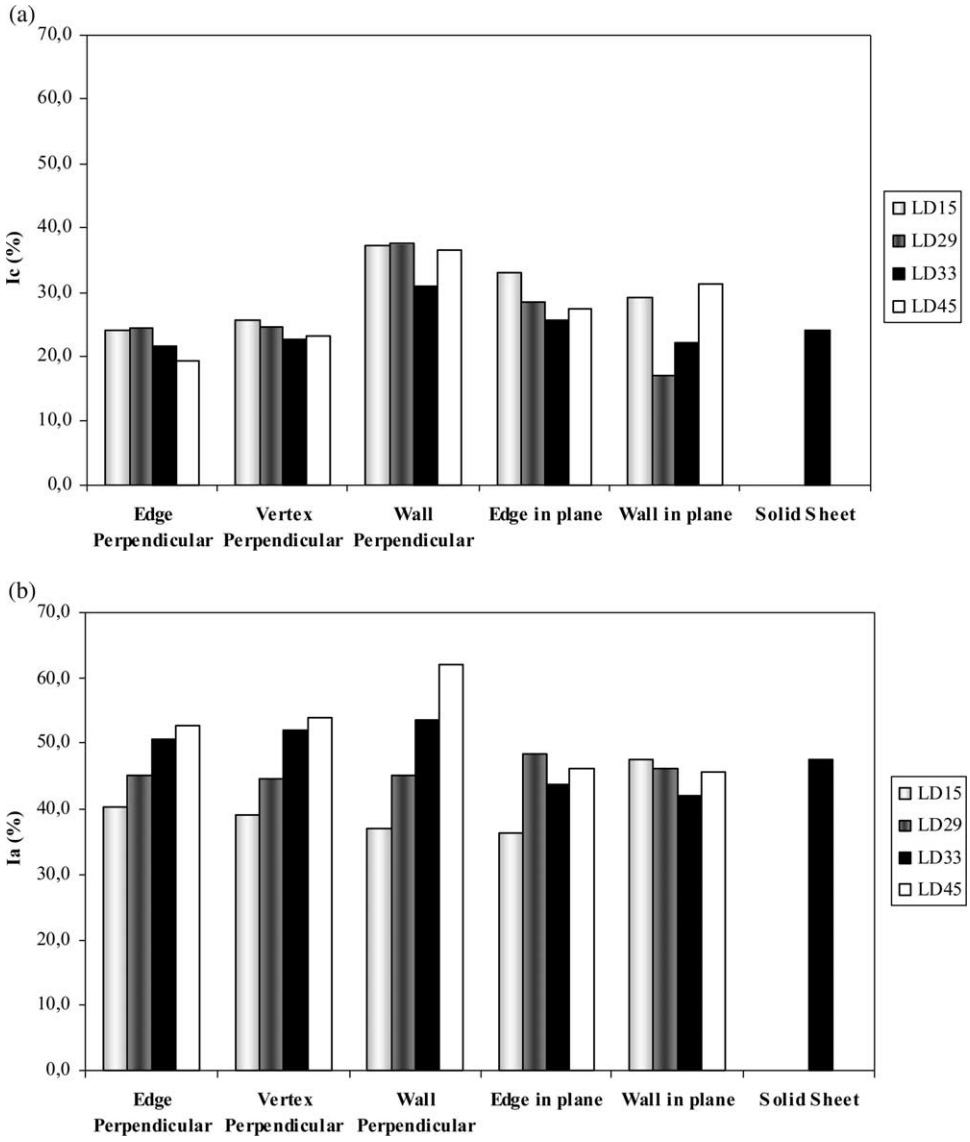

Fig. 8. Relative intensities for the (a) crystalline and (b) amorphous bands for the LD foams and the LD solid sheet.

The material with a more intense crystalline ban is the HD30 foam, followed by the HL34, LD33 and VA25 foams. This trend is true for all the foams elements and for the two measurement directions.

Fig. 8 shows the results as a function of the foam density. As it can be observed there is no evidence of a clear effect on the crystalline band; however, the amorphous band intensity slightly increases when the density rises. The foam density is a property which encompasses the different characteristics of the cellular structure (cell face thickness, cell size, mass fraction in the edges, cell shape, etc) the results seem to indicate that the cellular structure have an influence on the way the foam crystallises giving materials which a slightly different polymer morphologies depending on these characteristics. One possible explanation would be related to the different biaxial extension of foams of different densities. Other aspect which could have some influence is the different thermal conductivities of foams with different densities. Low density foams are better thermal insulators [33], therefore the cooling of these materials after foaming is slower than that of foams with higher densities, therefore the foams with higher densities could have a higher proportion of amorphous phase.

As it was pointed out in the introduction these kind of relationship between cellular structure and polymer morphology has been previously observed [14] using SEM on the etched surfaces of the foams.

5. Summary and conclusions

Micro-Raman spectroscopy has been shown to be a powerful technique to analyse the spatial homogeneity of the polymer morphology. Given the 1 μm^2 spatial resolution with which Raman spectra can be taken, it was determined that the observed Raman spectra strongly depend on the foam element under analysis.

The morphology of the crystalline phase of the polymeric matrix within the different elements (face, edges and vertex) is not homogeneous. The result for the crystalline band shows that cell faces are highly oriented and present a different morphology than that of edges and vertex. This effect is more prominent for materials of higher crystallinity (HDPE and blends of HDPE and LDPE).

On the other hand, the behaviour for the amorphous band allows concluding that, in general, this phase does not present a significant orientation and it is homogenously distributed in the different foam elements.

The previous differences seem to correlate well with orientation and phases proportion. Cell faces are strongly biaxial stretched during foaming, this could be the source of a higher level of chains packing and as a consequence a change in the crystalline content.

In addition, it has been shown that the solid sheets from which the foams are produced have a different morphology compared with that of the foams; this effect is more significant for polymers of higher crystallinity, such as HDPE. For these materials the polymer in the foam reduces its degree of order in comparison with the polymer in the solid sheet. For the branched materials (LDPE and EVA) the differences between solid sheets and foams are smaller.

Finally, it has been shown that the cellular structure could have an influence on the final polymer matrix morphology; in particular, it has been shown that the amorphous band increases its intensity when the density rises. This is an interesting topic in which a deeper study would be necessary and very attractive.

Regarding the understanding and prediction of the physical properties of foams these results are essential. The use of the physical properties of a solid sheet as parameters to compute the physical properties of foam is not an adequate approach, especially for linear polyolefins, in which the properties of the polymeric matrix could be very different to that of the solid sheet.

Acknowledgements

Financial assistance from the Local Government (Junta de Castilla y León, VA26/03), the Spanish Ministry of Science and Technology (MAT 2003/06797) and the Spanish Program for University Professors Mobility (M.A. Rodríguez-Pérez) (Spanish Ministry of Science and Education) is gratefully acknowledged.

References

[1] Gibson LJ, Ashby MF. Cellular solids: structure and properties. Oxford: Pergamon Press; 1988.
[2] Hilyard NC, Cunningham A. Low density cellular plastics: physical basis of behaviour. London: Chapman & Hall; 1994.
[3] Klempner D, Firsch C, editors. Polymeric foams. Munich: Hanser Publishers; 1991.
[4] Kumar VA, Seeler KA. Cellular and microcellular materials. vol. 53. New York: The American Society of Mechanical Engineers; 1994.
[5] Leach AG. J Phys D: Appl Phys 1993;26:733–9.
[6] Colishaw PG, Evans JRG. J Mater Sci 1994;29:486–98.
[7] Williams RJJ, Aldao CM. Polym Eng Sci 1983;23:32–40.
[8] Bedeaux D, Kapral R. J Chem Phys 1983;79:1783–9.
[9] Mills NJ, Gilchrist A. Cell Polym 1997;16:87–95.
[10] Clutton EQ, Rice GN. Cell Polym 1992;11:429–40.
[11] Almanza OA, Masso-Moreu Y, Mills NJ, Rodríguez-Pérez MA. J Polym Sci Part B: Polym Phys 2004;42:3741–9.
[12] Mills NJ, Zhu H. J Mech Phys Solids 1999;47:669–75.
[13] Kraynik AM, Neilsen MK, Reinelt DA, Warren WE. Foam micromechanics. In structure and rheology of foams, emulsions and cellular solids. In: Sadoc F, Rivier N, editors. Foams and emulsions. NATO ASI Series. Dordrecht, The Netherlands: Kluwer Academic Publishers; 1999. p. 259.
[14] Almanza OA, Rodríguez-Pérez MA, de Saja JA. Polymer 2001;42:7117–26.
[15] Sims GLA, Khunniteekool C. Cell Polym 1994;13:137–46.
[16] Rodríguez-Pérez MA, de Saja JA. J Macromol Sci Phys 2002;B41:761–75.
[17] Zipper P, Djoumaliisky S. Macomol Symp 2002;181:421–8.
[18] Almanza O, Rodríguez-Pérez MA, Chernev B, de Saja JA, Zipper P. Eur Polym J 2005;41:599–609.
[19] Snyder RG. J Chem Phys 1967;47:1316–60.
[20] Gall MJ, Hendra PJ, Peacock CJ, Cudby MEA, Willis HA. Spectrochim Acta 1972;28A:1485–96.
[21] Snyder RG, Hsu SL, Krimm S. Spectrochim Acta 1978;34A:395–406.
[22] Kobayashi M, Tadokoro H, Porter RS. J Chem Phys 1980;73(8):3635–42.
[23] Lafrance CP, Chabot P, Pigeon M, Prud'homme RE, Pezolet M. Polymer 1993;34:5029–37.
[24] Citra MJ, Chase DB, Ikeda RM, Gardner KH. Macromolecules 1995;28:4007–12.
[25] Ströbl CR, Hagedorn W. J Polym Sci Polym Phys Ed 1978;16:1181–93.
[26] Glotin M, Mandelkern L. Colloid Polym Sci 1982;260:182–92.
[27] Naylor CC, Meier RJ, Kip BJ, Williams KPJ, Mason SM, Conroy B, et al. Macromolecules 1995;28:2968–78.
[28] Mutter R, Stille W, Ströbl G. J Polym Sci Polym Part B: Polym Phys 1993;31:99–105.
[29] Stribeck N, Alamo RG, Mandelkern L, Zachmann HG. Macromolecules 1995;28:5029–36.
[30] Choi C, Bailey L, Rudi A, Pintar MM. J Polym Sci Polym Part B: Polym Phys 1997;35:2551–8.
[31] Mandelkern L, Alamo RG, Kennedy MA. Macromolecules 1990;23:4721–3.
[32] Lagarón JM, Dixon NM, Reed W, Pastor JM, Kip BJ. Polymer 1999;40:2569–86.
[33] Almanza OA, Rodríguez-Pérez MA, de Saja JA. Cell Polym 1999;18(6):385–401.